

2019

## Comparison between Numerical, Analytical, and Field Solutions with Experimental Data for 90° Open Channel Junctions

Ahmed Zahran, Tamer A. Gado, Ebrahim Rashwan

Follow this and additional works at: <https://digitalcommons.aaru.edu.jo/erjeng>

---

### Recommended Citation

Zahran, Tamer A. Gado, Ebrahim Rashwan, Ahmed (2019) "Comparison between Numerical, Analytical, and Field Solutions with Experimental Data for 90° Open Channel Junctions," *Journal of Engineering Research*: Vol. 3: Iss. 3, Article 6.

Available at: <https://digitalcommons.aaru.edu.jo/erjeng/vol3/iss3/6>

This Article is brought to you for free and open access by Arab Journals Platform. It has been accepted for inclusion in Journal of Engineering Research by an authorized editor. The journal is hosted on [Digital Commons](#), an Elsevier platform. For more information, please contact [rakan@aar.edu.jo](mailto:rakan@aar.edu.jo), [marah@aar.edu.jo](mailto:marah@aar.edu.jo), [u.murad@aar.edu.jo](mailto:u.murad@aar.edu.jo).

# Comparison between Numerical, Analytical, and Field Solutions with Experimental Data for 90° Open Channel Junctions

Ahmed Zahran<sup>1</sup>; Tamer A. Gado<sup>2</sup> and I. M. H. Rashwan<sup>3</sup>

<sup>1</sup> Director of Affairs, Ministry of Water Resources and Irrigation, Ph. D. Student, (e-mail: lordahmedz@gmail.com)

<sup>2</sup> Assistant Professor, is with Irrigation and Hydraulic Engineering Department, Faculty of Engineering, Tanta University, Tanta, Egypt, (e-mail: tamer.gado@f-eng.tanta.edu.eg; tamergado@hotmail.com)

<sup>3</sup> Hydraulic Professor, is with Irrigation and Hydraulic Engineering Department, Faculty of Engineering, Tanta University, Tanta, Egypt, (e-mail: ibrahim.rashwan@f-eng.tanta.edu.eg, [imh\\_rashwan@yahoo.com](mailto:imh_rashwan@yahoo.com))

**Abstract-** Junction in open channel flow points out any side water secession from natural or artificial channels. In the last decades, comprehensive theoretical and experimental investigations on the dividing flow in open channel junctions have been executed to understand the characteristics of this separating flow. In this research, a three-dimensional turbulence model by fluent software used to replicate the flow characteristics of a 90° open channel junctions for two geometries. One is with equal width and horizontal bed and the other is field canal junction with irregular section. The modeling is based on the Navier-Stokes equation and  $\kappa\text{-}\omega$  turbulent model. Comparing prepared to the numerical solution, the analytical model and the field works with published experimental data. The comparison showed that the numerical solution gave good agreements with maximum discrepancy 1.620% for rectangular sections and 0.718% for irregular sections than the published experimental data. The analytical solution gave a large error than numerical with a maximum discrepancy of 2.95% for the rectangular section and 11.485% for irregular sections than the published experimental data. A proposed relation between discharge ratio with upstream Froude number and depth ratio for the irregular section is suggested. The proposed equation has a maximum discrepancy equal to 0.433% with reference to the field data recorded.

## I. INTRODUCTION

The flow at any side water secession from rivers or main channels is called open-channel Junction flow which is an important aspect in hydraulic engineering. It has been studied in recent decades and still collect the attention of water resources engineering researchers as it is commonly existing in many water engineering projects. A tremendous number of authors have studied the characteristics of dividing flow theoretically, experimentally, and numerically. The primary objective of elementary researchers was to investigate the flow characteristics, such as diversion flow discharge and regimes. Taylor [1] investigated ways to estimate a flow discharge in the branch channel and suggested an empirical relationship between the quantity and depth ratios. Posterior research on the dividing flow influenced by the recent exploration of theoretical equations as Ramamurthy [2], Hager [3], Rashwan [4], and Rashwan and Saafan. [5]. The proposed equations by Rashwan [4] are inclusive with most of the factors neglected in other theoretical equations. The exact solution for that problem could not be revealed because of the depth variation upon the branch entrance and the unknown quantities like moment transfer from main to branch channel. Kesserwani et al. [6] collected the common defects

of all these models as:

- The theoretical dividing models necessitated a prior knowledge of the flow regime, which is not obvious to be determined without making additional assumptions that can't be applicable.
- During practical event applications like a storm, flooding may change the flow regime from one to another.
- Theoretical dividing models may fail to be performed because of a nonlinear computational complexity.

In the last decade, as a result of the advances in computer technology, many programs have been invented to conduct different types of numerical models describing branching channel flow. The first three-dimensional approach to the prediction flow characteristics 90° open channel junction with equal width conducted by Issa et al. [7]. The experimental observations carried out by Hsu et al. [8]. On dividing flows in a 90° rectangular equal width open-channel junction with a horizontal bed presented a depth-discharge relationship. Table (I) summarizes the typical properties of the numerical models used to simulate dividing junction flow, References from [9] to [18]. The fractional volume of fluid is the keynote of the (VOF) technique which is more flexible and efficient than other methods for treating complicated free boundary configurations with a minimum of stored information as shown by Hirt et al. [19]. Turbulent flows simulated usually used the standard  $K\text{-}\epsilon$  which independently determines the turbulent kinetic energy and dissipation rate by solving two separate equations Shamloo and Brzidaa.[20].

The objective of this paper is to examine a 3D numerical model to reproduce the flow characteristics of a 90° open channel junction. The performance of this model is evaluated by comparing its outputs with three different data: (1) the field data obtained from a selected typical Egyptian canal with dividing flow junction, (2) the published experimental data of Hsu et al. [8], and (3) the results of the analytical model obtained by Rashwan [4].

## II. FIELD WORK

A total of 15 discharge measurements at just three cross-sections were made covering a broad range of the Shemi canal flow which is located at a typical Egyptian canal at the North of El Mahalla El Kubra. The water depths, the real widths, the bed slope of reach and the flow discharge were measured by the Flow Tracker (a single-point Doppler current meter). Measures carried out to ensure the stability of the flow in a

steady state. The recorded measurements for the Shemi canal are tabulated in Table (2). Letters A, B, C, D and E represented experimental cases. Subscript (i, ii, and iii)

indicate the main canals upstream sections, the main canals downstream sections and the branch canals downstream sections, respectively.

TABLE I  
TYPICAL PROPERTIES OF NUMERICAL EXPERIMENTS

Researcher	Main channel			Branch channel				Numerical methods		
	Channel length (cm)	Channel Width (cm)	Channel depth (cm)	Channel length (cm)	Channel Width (cm)	Channel depth (cm)	Distant from inlet (cm)	Maximum discharge (liter/s)	Sells number	Numerical or turbulent model
Ramamurthy et al. [9]	310	61	30.5	244	61	30.5	279	47	–	RANS and k- $\omega$
Shamloo et al. [10]	600	30	25	300	30	25	300	–	–	RSM and K- $\epsilon$
Hedayat et al. [11]	275	15	31	168	15	31	100	11	137000	RSM
Farzin et al. [12]	450	30	–	120	30	–	300	12	5388	Saint-Venant equations
Neary et al. [13]	20W	W	2W	12W	W	2W	8W	–	–	RANS and k- $\omega$
Goudarzizadeh et al. [14]	274	15	31	168	15	31	100	11	200500	RANS and k- $\omega$
Momplot et al. [15]	490	30	20	260	30	20	200	8	700000	RANS
Li et al. [16]	1200	15	31	400	15	31	535	5.4	–	RANS
Seyedian [17]	800	25	70	225	20	70	550	–	–	SSIIM 2 and RNG K- $\epsilon$
Vasquez [18]	450	20	–	250	20	–	–	5	6066	River2D

TABLE II  
MEASUREMENTS OF GEOMETRIC PROPERTIES AND DISCHARGES FOR SHEMI CANAL

Run	Q <sub>i</sub> (l/s)	A (m <sup>2</sup> )	T(m)
Ai	3.431	9.512	13.032
Bi	5.054	13.929	13.739
Ci	6.917	18.589	14.505
Di	9.057	23.505	15.290
Ei	11.328	28.625	16.207
Aii	2.582	7.979	9.757
Bii	3.832	11.379	10.860
Cii	5.281	15.115	11.781
Dii	6.963	19.207	13.019
Eii	8.754	23.599	14.008
Aiii	0.848	3.085	3.747
Biii	1.222	4.593	5.392
Ciii	1.636	6.621	6.900
Diii	2.094	9.128	8.294
Eiii	2.574	12.047	9.667

### III. NUMERICAL MODEL

FLUENT (version 19) a commercial Computational Fluid Dynamics (CFD) software for modeling the fluid flow is used in the present study. Fluent solves the Navier-Stokes equation by three-dimensional Finite-Volume Method (FVM). Numerical solution subsequent comparison with experimental results showed that the FLUENT software is an effective tool for simulating the flow through the branching channel. On the other side, Neary et al. [13] used the k- $\omega$  turbulent model to develop a three-dimensional model for dividing flows in an open-channel T-diversion. The k- $\omega$  turbulence model was applied in the present study.

#### A. Governing Equations

The mass conservation equations are the basic governing formularization for numerical modeling of flows. Consider an element of so small size dx, dy, and dz in the flow, the mass flow rate across a face of the element expressed by the product of density, area and the velocity component normal to the face.

By considering the viscous stresses expressed as functions of strain rate in three dimensions, Pavanelli [10] presented the Navier-Stokes equations (for compressible fluids with inconstant viscosity) in the x-direction as the following:

$$\rho \frac{Du}{Dt} = \frac{\partial p}{\partial x} + \frac{\partial}{\partial x} \left( 2\mu \frac{\partial u}{\partial x} + \lambda \text{div}(u) \right) + \frac{\partial}{\partial y} \left( \mu \frac{\partial u}{\partial y} + \frac{\partial v}{\partial y} \right) + \frac{\partial}{\partial z} \left( \mu \frac{\partial u}{\partial z} + \frac{\partial w}{\partial y} \right) + S_{MX} \quad (1)$$

where  $\rho$  is density;  $p$  is the pressure;  $(u, v, w)$  are scalar velocities in the  $x, y,$  and  $z$ -direction;  $\mu$  is the dynamic viscosity, and  $S_{MX}$  is a term expresses the body forces effect of  $x$ -momentum per unit discharge. In the same way, the Navier-Stokes equations in the  $y$ -direction and the  $z$ -direction was obtained.

#### B. Numerical Solution for Chung-Chieh junction

Experimental data of Hsu et al [8] used for validating the numerical approaches. Numerical solution for Hsu et al junction can be carried out as follows:

##### Hsu junction domain and mesh

According to Hsu et al [8] junction model was designed as shown in Figure 1. The canal has an equal width of 0.147m, and the length of the main channel and the side branch considered 2.147 m and 1m, respectively. The solution

domain was divided into 756000 polyhedral cells as shown in Figure 2.

#### Hsu junction Boundary Conditions

Mass flow inlet, outflow, and outlet vent boundary conditions are specified at the main canal inlet and the outlet at main and branch channel outlet respectively. The velocity is specified to be zero at the solid boundaries.

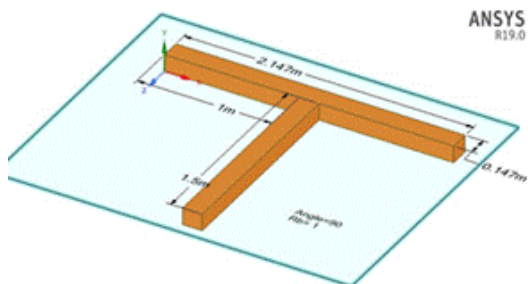


Figure 1. Numerical model geometry for Hsu et al [8] junction

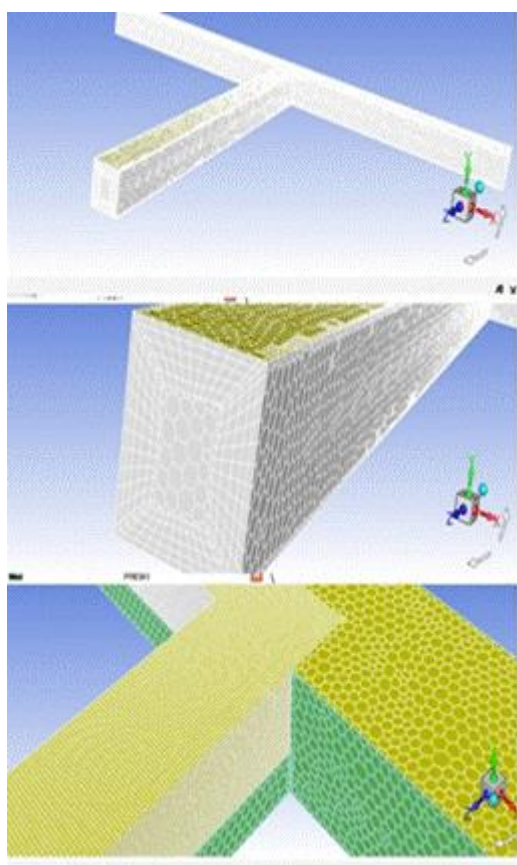


Figure 2. Hsu et al [8] junction computational mesh

#### C. Numerical solution to Shime junction

The cross-section of the main canal and branch for the Shemi canal adopted in the numerical simulation whereas the length of the main channel and the side branch considered 100 m and 50 m respectively.

#### Shemi junction domain and mesh

Triangular cells used in initial grids. Reinforcements were performed by making finer zones around the branch instance

and inflations beside channels bed and banks. Mesh sizing method used to achieve a finer layer around the prospective water surface. Furthermore, all elements were converted to polyhedral cells of different sizes by using fluent meshes. Figure 3, shows details of the computational mesh of Shemi junction. The solution domain was divided into 684,442 polyhedral cells.

#### Shemi junction Boundary Conditions

Mass flow inlet, outflow, and outlet vent boundary conditions are specified at the main channel inlet and the outlet at main and branch channel outlet respectively. Non-slip boundary conditions are set at the solid boundaries it indicates that the fluid sticks to the wall and moves with the same zero velocity as the wall, Gandhi et al. [21]. The best result occurs when the sand-grain roughness height  $K_s = 0.01$  is specified to model the roughness effects. The water surface of all geometry is set as Mass flow inlet with zero mass flow value. Five flows are considered to the inlet equal to the field measurement at the upstream main channels whereas the field geometry survey is applied to the upstream main channel inlet and the branch canal outlet.

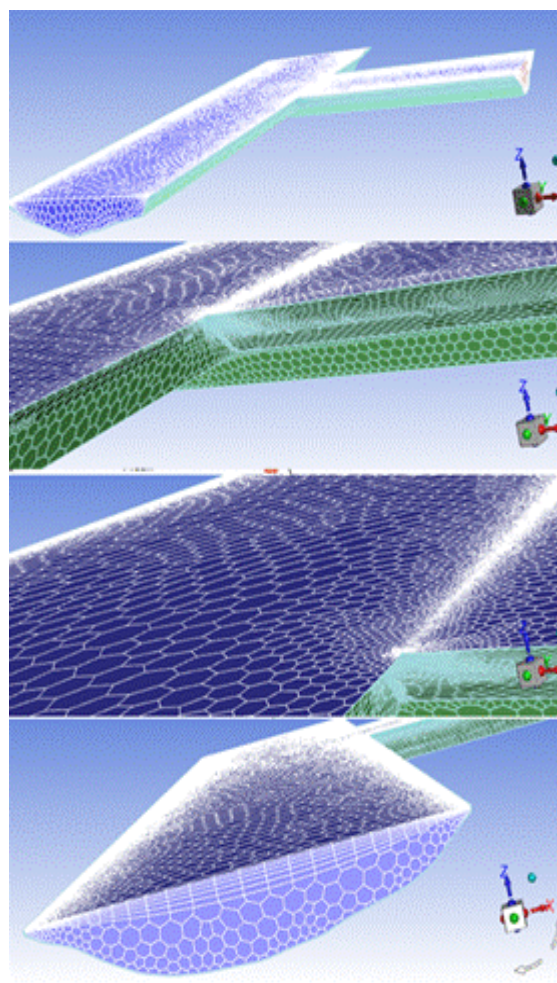


Figure 3. Shime junction computational mesh

#### D.. Convergence for the numerical solution

In the rectangular numerical model, Convergence accuracy is obtained when normalized calculation residuals are below  $10^{-6}$ . Time steps used varied from 0.001 s to 0.01 s and the dynamic steady state is achieved after about 40 s.

Whereas, convergence in field simulating is obtained when normalized calculation residuals are below  $10^{-4}$ . Time steps used varied from 0.0005 s to 0.01 s and the time to reach a dynamic steady state achieved after about 127 s. During this process, the results for each time-step are displayed. Figure 4, includes the number of iterations required, the maximum residual.

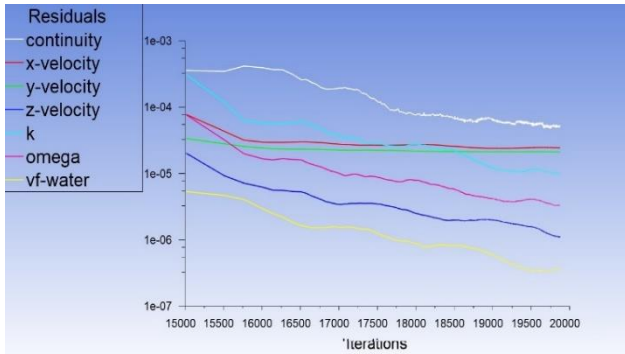


Figure 4. Scaled equations residuals of the numerical model

IV. ANALYTICAL MODEL

Rashwan [4] developed the subcritical steady dividing flows in open channel junctions as:

$$\frac{F_1^2 R_q^2 R_y}{R_b} - R_q F_1^2 = \frac{R_q}{2} - \frac{R_b}{R_y^2} - 0.5(R_b - R_q) \left( 1 + \frac{F_1^2}{3} + \frac{F_1^4}{20} \right) + \left( \frac{R_q + R_b/R_y}{2} \right) \left( \frac{L_1}{y_1} S_{01} \right) - \frac{F_1^2 L_1}{2C^2 y_1} \left( \frac{R_q + R_b}{2} + \frac{y_1}{b_1} \right) + \left( \frac{R_q^2 R_y}{R_b^2 \left( R_b R_y + \frac{2y_1}{b_1} \right)} \right) \quad (2)$$

where  $F_1$  is the upstream Froude number,  $R_q$  is the relative discharge,  $R_y$  is the upstream-to-downstream depth ratios  $R_y = y_1/y_2$ ,  $R_b$  is the upstream-to-downstream widths ratios  $R_b = b_2/b_1$ ,  $y_1$  is the upstream water depth,  $y_2$  is the downstream water depth,  $b_1$  is the upstream width,  $b_2$  is the downstream width,  $L_1$  and  $L_2$  are the lengths of the control volume 1 and 2,  $S_{01}$  and  $S_{02}$  are the averages of bed slopes of the main and branch channel, and  $C$  is the dimensionless Chezy coefficient.

Replacing the upstream-to-downstream widths ratios ( $R_b = b_2/b_1$ ) with the upstream-to-downstream top widths ratios ( $R_T = T_2/T_1$ ), and the upstream-to-downstream depth ratios ( $R_y = y_1/y_2$ ) with the upstream-to-downstream hydraulic depth ratios ( $R_{yh} = y_{h1}/y_{h2}$ ) the model was acceptable to use in the field. Eq. (2) can be written as follows:

$$\frac{2F_1^2 R_q^2 R_{yh}}{R_T} - (1 - R_q) F_1^2 = \frac{1 - R_q}{2} - \frac{R_T}{R_{yh}^2} - 0.5(R_T - R_q) \left( 1 + \frac{F_1^2}{3} + \frac{F_1^4}{20} \right) + \frac{F_1^2 L_1}{2C^2 y_1} \left( \frac{(1 - R_q) + (R_T/R_{yh})}{2} + \frac{y_1}{b_1} \right) + \left( \frac{R_q^2 R_{yh3}}{R_T^2 \left( R_T R_{yh} + \frac{2y_1}{b_1} \right)} \right) \quad (3)$$

where  $R_{yh}$  = the upstream-to-downstream hydraulic depth ratios,  $R_{yh} = y_{h1}/y_{h2}$  and  $R_T$  = the upstream-to-downstream top widths ratios,  $R_T = T_2/T_1$

V. RESULTS, ANALYSIS, AND DISCUSSIONS

Comparison between the analytical and numerical models with values corresponding experimental data from Hsu et al. [8] are shown in Table III where the discrepancy was computed as follow:

$$\text{Discrepancy \%} = \left( \frac{R_{y, \text{experimental}} - R_{y, \text{analytical}}}{R_{y, \text{experimental}}} \right) \times \% \quad (4)$$

TABLE III

COMPARISON BETWEEN THE NUMERICAL AND ANALYTICAL DEPTH RATIO VALUES AND THE CORRESPONDING EXPERIMENTAL DATA IN A RECTANGULAR CHANNEL

Run No.	$R_y$ Hsu et al. [8]	$R_y$ Analytical Eq. (2)	Discrepancy %	$R_y$ Numerical	Discrepancy %
1	0.925	0.924	0.11	0.918	0.76
2	0.935	0.926	0.99	0.922	1.39
3	0.905	0.878	2.95	0.896	0.99
4	0.889	0.881	0.98	0.881	0.92
5	0.958	0.953	0.55	0.949	0.94
6	0.950	0.948	0.24	0.935	1.62
7	0.939	0.938	0.17	0.925	1.49
8	0.947	0.943	0.43	0.941	0.63
9	0.960	0.958	0.15	0.952	0.83
10	0.963	0.965	0.23	0.960	0.27
11	0.950	0.958	0.82	0.941	0.95
12	0.950	0.956	0.62	0.955	0.53

The calculated values of the main canal depth ratios by proposed analytical and numerical models shown in Table III were found in a good agreement with the Hsu et al. [8] data. Also, the comparison between numerical and analytical depth ratio with values for Shemi canal field measurements shown in Table IV.

TABLE IV

COMPARISON BETWEEN NUMERICAL AND ANALYTICAL DEPTH RATIO VALUES FOR SHEMI CANAL FIELD MEASUREMENTS

Run No.	$R_{yh}$ Fieldworks	$R_{yh}$ Analytical Eq. (3)	Discrepancy %	$R_{yh}$ Numerical	Discrepancy %
A	0.893	0.995	11.485	0.899	0.718
B	0.968	0.995	2.805	0.971	0.351
C	0.999	0.996	0.275	0.998	0.069
D	1.042	0.996	4.371	1.036	0.546
E	1.048	0.997	4.915	1.042	0.614

The calculated values of the main canal depth ratios by proposed numerical models shown in Table IV were found in a good agreement with fieldwork measurements. While the main canal depth ratios by proposed analytical models were found with a big discrepancy in one case and a moderate discrepancy with two cases and a good discrepancy with two cases.

Relationship between the upstream Froude number ( $F_{r1}$ ) to the separated discharge ( $1 - R_q$ )

Figure (5) shows the measurements of the upstream Froude

number ( $F_{r1}$ ) to the separated discharge ( $1-R_q$ ) for Hsu junction. The relationship may be expressed as follows:

$$R_q = -3.202(F_{r1})^2 + 4.4997F_{r1} - 0.7249 \dots\dots\dots (5)$$

With a coefficient of determination  $R^2$  equal to 0.8937,

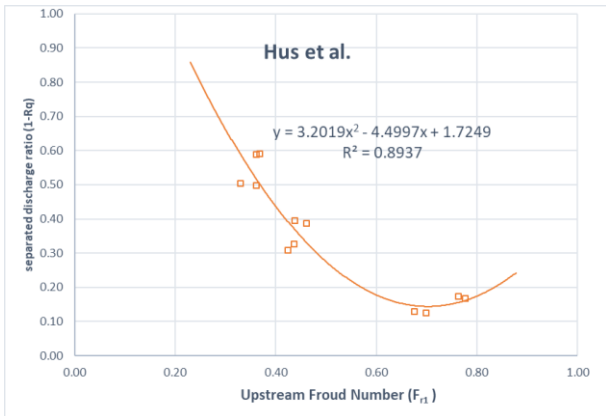


Figure (5) Effect of upstream Froude number on the separated discharge for Hsu junction

A nonlinear regression analysis conducted using (SPSS) program to suggest relations between discharge ratio, upstream Froude number, and depth ratio as follows:

$$R_q = 93.972 F_{r1}^4 - 207.772 F_{r1}^3 + 162.637 F_{r1}^2 - 51.197 F_{r1} + 56.468 R_y^3 - 50.884 R_y^2 - 45.813 R_y + 46.895 \dots\dots (6)$$

With a coefficient of determination  $R^2$  equal to 0.981.

Figure (6) shows the field measurements of the upstream Froude number ( $F_{r1}$ ) to the separated discharge ( $1-R_q$ ) for the Shime canal junction. The relationship of the field measurements of the upstream Froude number ( $F_{r1}$ ) to the separated discharge ( $1-R_q$ ) for Shime canal junction may be expressed as follows:

$$R_q = -0.4881F_{r1} + 0.8168 \dots\dots\dots (7)$$

With a coefficient of determination  $R^2$  equal to 0.9287

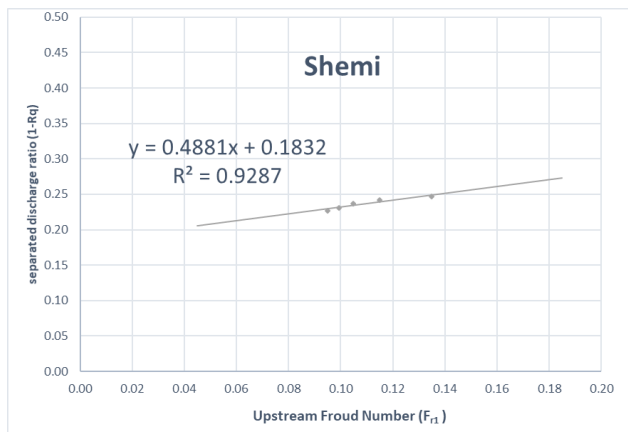


Figure (6) Effect of upstream Froude number on the separated discharge for Shemi junction

Also, a regression analysis conducted using (SPSS) program to suggest relations between discharge ratio, upstream Froude number, and depth ratio as follows:

$$R_q = 1.626F_{r1} + 5.739R_y - 5.566 \dots\dots\dots (8)$$

With a coefficient of determination  $R^2$  equal to 0.937.

A comparison between the predicted values of the Eq. (6) and corresponding experimental data for Hsu et al. [8] are given in Table (v) with minimum and maximum discrepancy equal -0.014% and 5.065% respectively.

TABLE V  
COMPARISON BETWEEN DISCHARGE RATIO FOR HSU ET AL. [8] JUNCTION FROM THE FIELD DATA AND CALCULATED BY EQ. (6)

Run	$R_q$ Hsu et al. [8]	$R_q$ Proposed Eq. (6)	Discrepancy %
1	0.875	0.840	3.960
2	0.871	0.900	-3.339
3	0.833	0.833	-0.014
4	0.826	0.827	-0.068
5	0.692	0.689	0.490
6	0.674	0.640	5.065
7	0.613	0.618	-0.821
8	0.604	0.615	-1.840
9	0.503	0.517	-2.689
10	0.496	0.484	2.515
11	0.411	0.403	2.030
12	0.409	0.422	-3.238

The comparison between the predicted values of the equation (8) and corresponding experimental data for Hsu et al. [8] are given in Table (vi) with minimum and maximum discrepancy equal - 0.126% and 0.433% respectively.

TABLE VI  
COMPARISON BETWEEN DISCHARGE RATIO FOR SHEMI CANAL FROM THE FIELD DATA AND CALCULATED BY EQ. (8)

Run	$R_q$ Field Data Shemi junction	$R_q$ Proposed Eq. (8)	Discrepancy %
A	0.753	0.752	-0.126
B	0.758	0.761	0.433
C	0.764	0.765	0.132
D	0.769	0.771	0.205
E	0.773	0.771	-0.235

## VI. CONCLUSIONS

The flow distribution in a 90° horizontal bed open channel junction for both equal width and irregular section has been studied numerically, analytically and field data for subcritical flow using data from published experimental data. The numerical model based on the FLUENT (version 19) a commercial Computational Fluid Dynamics (CFD) software. The analytical model based on the model suggested by Rashwan [4]. The comparison made depending on published experimental data of Hsu et al [8] and field works. The SPSS program is used to estimate general equations to analyze discharge values related to the upstream Froude number, and depths ratio with suitable discrepancy percentage. The conclusions can be presented as:

### A. For junction with rectangular sections

- The numerical solution appeared good similarity to the published experimental data by Hsu et al. [8] with minimum and maximum discrepancy equal to 0.27% and 1.62%.

- The analytical model predicted values good agreement with the same experimental data with minimum and maximum discrepancy equal to 0.11% and 2.95% respectively.

#### B. For junction with irregular sections

- The minimum and maximum discrepancy was 0.07% and 0.72% in the numerical model whereas the minimum and the maximum discrepancy was 0.28% and 11.49% in the analytical model.
- Equation (Eq. (8)) for discharge ratio, upstream Froude number, and depth ratio appeared minimum and maximum discrepancy equal to -0.126% and 0.433% respectively with the field works data.

#### REFERENCES

- [1] V. Te Chow, "Open channel flow," London: McGRAW-HILL, Vol. 11, No. 95, pp. 99–136, 1959.
- [2] A. S. Ramamurthy, D. Minh Tran, and L. B. Carballada, "Dividing flow in open channels," *Journal Hydraulic Engineering*, Vol. 116, No. 3, pp. 449–455, 1990.
- [3] W. H. Hager, "Supercritical flow in channel junctions," *Journal Hydraulic Engineering*, Vol. 115, No. 5, pp. 595–616, 1989.
- [4] I. M. H. Rashwan, "Dynamic Model for Subcritical Dividing Flows in Open Channel Junction," in *Proc. of 8th Int. Water Tech. Conf., IWTC*, 2004.
- [5] I. M. H. Rashwan and T. A. Saafan, "Dividing Flow at a 90-degree Open Channel Junction, Dividing Flow at a 90-degree Open Channel Junction."
- [6] G. Kesserwani, J. Vazquez, N. Rivière, and Q. Liang, "1D computation of open-channel flow division at a 90o intersection," *Journal Hydraulic Engineering*, Vol. 116, No. 3, pp. 449–456, 2008.
- [7] R. I. Issa and P. J. Oliveira, "Numerical prediction of phase separation in two-phase flow through T-junctions," *Comput. Fluids*, Vol. 23, No. 2, pp. 347–372, 1994.
- [8] C.-C. Hsu, C.-J. Tang, W.-J. Lee, and M.-Y. Shieh, "Subcritical 90o equal-width open-channel dividing flow," *J. Hydraul. Eng.*, Vol. 128, No. 7, pp. 716–720, 2002.
- [9] A. S. Ramamurthy, J. Qu, and D. Vo, "Numerical and Experimental Study of Dividing Open-Channel Flows," *J. Hydraul. Eng.*, Vol. 133, No. 10, pp. 1135–1144, 2007.
- [10] H. Shamloo and B. Pirzadeh, "Numerical investigation of the velocity field in dividing open-channel flow," in *Proceedings of the 12th WSEAS International Conference on APPLIED*, 2007.
- [11] N. Hedayat and M. H. Tavana, "The consequences of varying the width ratio parameter of the lateral water intake structure to the main canal," *Bull. Env. Pharmacol. Life Sci*, Vol. 3, No. March, pp. 48–54, 2014.
- [12] M. Farzin, E. Alamatian, and R. Amini, "Finite volume modelings of flow in T-junction open channels," *7thSASTech 2013*, Iran, Bandar-Abbas., Vol. m, No. 1944, 2013.
- [13] V. S. Neary and F. Sotiropoulos, "Numerical investigation of laminar flows through 90-degree diversions of rectangular cross-section," *Comput. Fluids*, Vol. 25, No. 2, pp. 95–118, 1996.
- [14] R. Goudarzizadeh, N. Hedayat, and S. Jahromi, "Three-dimensional simulation of flow pattern at the lateral intake in a straight path, using the finite-volume method," *World Acad. Sci. Eng. Technol.*, Vol. 47, pp. 656–661, 2010.
- [15] A. Momplot, G. Lipeme Kouyi, E. Mignot, N. Rivière, and J. L. Bertrand-Krajewski, "Typology of the flow structures in dividing open-channel flows," *J. Hydraul. Res.*, Vol. 55, No. 1, pp. 63–71, 2017.
- [16] C. W. Li and C. Zeng, "3D Numerical modeling of flow divisions at open channel junctions with or without vegetation," *Adv. Water Resour.*, vol. 32, No. 1, pp. 49–60, 2009.
- [17] S. M. Seyedian, M. S. Bajestan, and M. Farasati, "Effect of bank slope on the flow patterns in river intakes," *J. Hydrodyn.*, vol. 26, No. 3, pp. 482–492, 2014.
- [18] J. A. Vasquez, "Two-dimensional numerical simulation of flow diversions," in *17th Canadian Hydrotechnical Conference: Hydrotechnical Engineering: Cornerstone of A Sustainable Environment*, Edmonton, Alberta, 2005.
- [19] C. W. Hirt and B. D. Nichols, "Volume of Fluid (VOF) method for the dynamics of free boundaries," *J. Comput. Phys.*, Vol. 39, No. 1, pp. 201–225, 1981.
- [20] H. Shamloo and B. Pirzadeh, "Investigation of characteristics of separation zones in T-junctions," *WSEAS Trans. Math.*, Vol. 7, No. 5, pp. 303–312, 2008.